Iranian Journal of Numerical Analysis and Optimization
Vol. 15, No. 1, 2025, pp 284–310
https://doi.org/10.22067/ijnao.2024.86799.1388
https://ijnao.um.ac.ir/

Research Article

Fitted tension spline method for singularly perturbed parabolic problem with a large temporal lag

S.K. Tesfaye*, T.G. Dinka, G.F. Duressa and M.M. Woldaregay

Abstract

We develop a fitted tension spline numerical scheme for singularly perturbed parabolic problems with a large temporal lag. A priori bounds and

*Corresponding author

Received 10 February 2024; revised 26 October 2024; accepted 27 October 2024

Sisay Ketema Tesfaye
Department of Mathematics, Hawassa College of Teacher Education, Hawassa, Ethiopia. e-mail: sisayk12@gmail.com

Tekle Gemmechu Dinka
Department of Applied Mathematics, Adama Science and Technology University, Adama, Ethiopia. e-mail: tekgem@yahoo.com

Gemechis File Duressa
Department of Mathematics, Jimma University, Jimma, Ethiopia. e-mail: gammeef@gmail.com

Mesfin Mekuria Woldaregay
Department of Applied Mathematics, Adama Science and Technology University, Adama, Ethiopia. e-mail: msfnmkr02@gmail.com

How to cite this article
Tesfaye,S.K., Dinka, T.G., Duressa, G.F. and Woldaregay, M.M., Fitted tension spline method for singularly perturbed parabolic problem with a large temporal lag. *Iran. J. Numer. Anal. Optim.*, 2025; 15(1): 284-310. https://doi.org/10.22067/ijnao.2024.86799.1388

properties of the continuous solution are discussed. Due to the problem's small parameter ε, as a multiple diffusion term, the solution possesses a multi-scale character in the boundary layer region, which is exhibited on the right side of the domain. This results in a challenging duty to solve such problems analytically or using classical numerical methods. Classical numerical methods cause spurious nonphysical oscillations unless an unacceptable number of mesh points is considered, which requires a high computational cost. To handle this difficulty, the method comprises the Crank–Nicolson method in the temporal direction and the fitted spline method in the spatial direction on uniform meshes. The stability of the method is studied using the discrete maximum principle and discrete solution bounds. We proved that the proposed scheme is uniformly convergent, with an order one in the space and an order two in the time directions. Two numerical examples are considered to validate the efficiency and applicability of the proposed scheme. Furthermore, the boundary layer behavior of the solutions is given graphically.

AMS subject classifications (2020): Primary 65M06; Secondary 65M12, 65M15.

Keywords: Singularly perturbed, Delay differential equation; Exponentially fitted finite difference; Tension spline; Uniform convergence.

1 Introduction

Delay differential equations in which its higher order derivative term is multiplied by a small perturbation parameter $(0 < \varepsilon \ll 1)$ and contains at least one delay parameter on the term different from the highest derivative term is known as singularly perturbed delay differential equations (SPDDEs); otherwise it is known as neutral delay differential equations. A singularly perturbed problem, which arises as a time delay, occurs in many application areas of science and engineering. A simplified example of a time-delayed mathematical model, which is used in the automatic control system of a furnace to produce metal sheets, is given as [26]

$$\frac{\partial z(s,t)}{\partial t} = \varepsilon \frac{\partial^2 z(s,t)}{\partial s^2} + v(g(z(s,t-\zeta)))\frac{\partial z(s,t)}{\partial s} + c[f(z(s,t-\zeta)) - z(s,t)], \quad (1)$$

where z denotes the temperature distribution in a metal sheet, and f and v denote the heat source and the velocity with which the metal sheet is moving, respectively. Both f and v are dependent on the term $z(s, t-\zeta)$. The time delay of fixed length ζ is induced because of the finite speed of the controlling device. The existence of perturbation parameter in the problem the solution exhibits a boundary layer. The boundary layer is an asymptotically narrow region located on the left side or right side of the domain depending on the sign of the convection term, where the solution has a steep gradient as ε tends to zero [1]. Due to the presence of this layer, one encounters computational difficulties in treating a singularly perturbed problem using analytical or classical numerical schemes [12]. Classical numerical schemes lead to spurious nonphysical oscillations in the numerical solution, unless an unacceptably large number of mesh points are considered, which leads to a massive computational cost [3]. In response to this stiffness behavior, different authors have to look for sounding numerical schemes, which converge uniformly regardless of ε.

Recently, Gowrisankar and Natesan [8] applied the upwind finite difference scheme on a piecewise uniform mesh. In [3, 7], a hybrid scheme of the midpoint upwind in the outer layer region and the central difference scheme in the layer region is proposed. In [4], the upwind finite difference method on Shishkin mesh is used. In [13, 14], an adaptive mesh refinement approach is employed using the concept of entropy function. An exponentially fitted finite difference scheme is used in [9, 25, 27]. The nonstandard finite difference scheme is considered by [2]. An exponentially fitted spline-based difference scheme is discussed in [15]. In [23], the authors proposed the Crank–Nicolson method in the time direction and the operator compact implicit (OCI) method on the Shishkin mesh in the space direction. The backward-Euler in the time direction and method of line following Micken's type discretization for the space derivatives are used in [16]. Podila and Kumar [20] used a stable finite difference method, which works on a uniform mesh and an adaptive mesh. Sahoo and Gupta [22] used a higher-order finite difference method with an identity expansion on a piecewise uniform mesh. The authors [12, 17] proposed the numerical schemes that work for both cases when the delay term is large or small. A fitted tension spline method for reaction-diffusion problem with negative shift is used in [5]. A robust numerical scheme for spatio-temporal delays problem is discussed in [6]. A nonuniform Haar wavelet method is discussed in [19].

To the best of the authors' knowledge, the fitted tension spline scheme has not been developed for solving singularly perturbed parabolic problems with a large temporal lag. As stated in [24], constructing uniformly convergent numerical methods regardless of ε is an active study area. This motivated us to look for a sounding numerical scheme that converges uniformly regardless of ε. In this study, we propose a numerical method that comprises the Crank–Nicolson scheme in the time direction and fitted tension spline scheme in the spatial direction on uniform meshes. Thus, the main objective is to develop a more accurate, stable, and uniformly convergent numerical scheme for singularly perturbed parabolic problems with a large temporal lag.

In this study, C is used as a generic positive constant that is independent of the mesh parameters and ε. The norm $\|\cdot\|$, denoted by $\|f\| = \max_{(s,t)\in\bar{\mathbb{D}}} |f(s,t)|$, is the maximum norm.

2 Continuous problem

On the rectangular domain $\mathbb{D} = \Omega \times \Lambda = (0,1) \times (0,\mathbb{T}]$, we consider a singularly perturbed problem of the form

$$\begin{cases} z_t(s,t) + \mathcal{L}_\varepsilon z(s,t) = -\mu(s,t)z(s,t-\zeta) + f(s,t), & (s,t) \in \mathbb{D}, \\ z(s,t) = \psi_b(s,t), & (s,t) \in \eta_b = [0,1] \times [-\zeta, 0], \\ z(0,t) = \psi_l(t), & on\ \eta_l = \{0\} \times [0,\mathbb{T}], \\ z(1,t) = \psi_r(t), & on\ \eta_r = \{1\} \times [0,\mathbb{T}], \end{cases} \tag{2}$$

where $\mathcal{L}_\varepsilon z(s,t) = -\varepsilon z_{ss}(s,t) + \kappa(s) z_s(s,t) + \gamma(s,t) z(s,t)$.

Moreover, $0 < \varepsilon \ll 1$ and $\zeta > 0$ are given constants, the functions $\kappa(s), \gamma(s,t), \mu(s,t)$,
$f(s,t)$ on $\bar{\mathbb{D}} = \bar{\Omega} \times \bar{\Lambda} = [0,1] \times [0,\mathbb{T}]$, and $\psi_b(s,t)$, $\psi_l(t)$, $\psi_r(t)$ on $\eta = \eta_l \cup \eta_r \cup \eta_b$, are sufficiently smooth and bounded that satisfy $0 < \varpi \leq \gamma(s,t)$, $0 < \theta \leq \mu(s,t)$, $0 < \beta \leq \kappa(s), (s,t) \in \bar{\mathbb{D}}$. Under these assumptions,

the solution of the problem (2) exhibits a boundary layer of width $O(\varepsilon)$ along $s = 1$ [3].

2.1 A priori bounds

The existence and uniqueness of the solution of (2) can be ensured by the sufficiently smoothness of $\psi_b(s,t)$, $\psi_l(t)$, $\psi_r(t)$, and the compatibility conditions of the corner points and the delay term [21], which are stated as

$$\psi_l(0) = \psi_b(0,0),\ \psi_r(0) = \psi_b(1,0), \tag{3}$$

$$\begin{aligned}
\frac{d\psi_l(0)}{dt} - \varepsilon\frac{\partial^2\psi_b(0,0)}{\partial s^2} + \kappa(0)\frac{\partial\psi_b(0,0)}{\partial s} + \gamma(0,0)\psi_b(0,0) = &-\mu(0,0)\psi_b(0,-\zeta)\\
&+ f(0,0),\\
\frac{d\psi_r(0)}{dt} - \varepsilon\frac{\partial^2\psi_b(1,0)}{\partial s^2} + \kappa(1)\frac{\partial\psi_b(1,0)}{\partial s} + \gamma(1,0)\psi_b(1,0) = &-\mu(1,0)\psi_b(1,-\zeta)\\
&+ f(1,0).
\end{aligned} \tag{4}$$

Taking $\varepsilon = 0$ in (2), we obtain reduced problem of the form

$$\begin{cases}
\frac{\partial z^0(s,t)}{\partial t} + \kappa(s)\frac{\partial z^0(s,t)}{\partial s} + \gamma(s,t)z^0(s) = -\mu(s,t)z^0(s,t-\zeta) + f(s,t),\\
z^0(s,t) = \psi_b(s,t), \qquad (s,t) \in \eta_b,\\
z^0(0,t) = \psi_l(t), \qquad t \in \bar{\Lambda},
\end{cases} \tag{5}$$

where $z^0(s,t)$ is reduced problem solution.

Lemma 1 (Maximum principle)**.** [3]Let $\phi(s,t) \in C^2(\mathbb{D}) \cap C^0(\bar{\mathbb{D}})$, given that $\phi(s,t) \geq 0$ for all $(s,t) \in \eta$ and $(\frac{\partial}{\partial t} + \mathcal{L}_\varepsilon)\phi(s,t) \geq 0$, for all $(s,t) \in \mathbb{D}$; then $\phi(s,t) \geq 0$, for all $(s,t) \in \bar{\mathbb{D}}$.

Lemma 2. [3, 7] Let $z(s,t)$ be the solution of (2); then the following estimate holds:

$$|z(s,t) - \psi_b(s,0)| \leq Ct, \qquad (s,t) \in \bar{\mathbb{D}}.$$

Lemma 3. [3, 7] The solution $z(s,t)$ of (2) is estimated as

$$|z(s,t)| \leq C, \qquad (s,t) \in \bar{\mathbb{D}}.$$

Lemma 4 (Stability result)**.** [12] The solution $z(s,t)$ of (2) is estimated as

$$\left|z(s,t)\right| \leq \varpi^{-1}\|f\| + \max\{|\psi_l(t)|, |\psi_b(s,t)|, |\psi_r(t)|\},$$

where $\varpi \leq \gamma(s,t)$.

Lemma 5. [3, 23] Let $z(s,t)$ be the solution of (2); then its derivative satisfies the estimate

$$\begin{aligned} \left|\frac{\partial^p z(s,t)}{\partial s^p}\right| &\leq C\left(1 + \varepsilon^{-p}\exp\left(\frac{-\beta}{\varepsilon}(1-s)\right)\right), \qquad (s,t) \in \bar{\mathbb{D}},\ p = 0(1)4, \\ \left|\frac{\partial^k z(s,t)}{\partial t^k}\right| &\leq C, \qquad (s,t) \in \bar{\mathbb{D}},\ k = 0(1)2, \end{aligned} \tag{6}$$

where $\beta \leq \kappa(s)$.

3 Numerical scheme

3.1 Temporal discretization

The time interval $[0,\mathbb{T}]$ is discretized uniformly with step size Δt as $\bar{\Lambda}_t^M = \{t_j = j\Delta t, j = 0,1,2,\ldots,M, t_M = \mathbb{T}, \Delta t = \mathbb{T}/M\}$ and $\bar{\Lambda}_t^m = \{t_j = j\Delta t, j = 0,1,2,\ldots,m, t_m = \zeta, \Delta t = \zeta/m\}$ with M mesh points in $[0,\mathbb{T}]$ and m mesh points in $[-\zeta, 0]$. We have $\mathbb{T} = r\zeta$ for some positive integer r. The approximation of $z(s,t)$ at the grid point $j+1$ is given as $Z^{j+1}(s)$. Using the Crank–Nicolson approach for semi-discretizing of (2), we get

$$\left(1 + \frac{\Delta t}{2}\mathcal{L}_\varepsilon{}^{\Delta t}\right)Z^{j+1}(s) \tag{7}$$

$$= \begin{cases} \left(1 - \frac{\Delta t}{2}\mathcal{L}_\varepsilon{}^{\Delta t}\right)Z^j(s) - \Delta t\mu(s,t_{j+1/2})\psi_b(s) \\ +\Delta t f(s,t_{j+1/2}), \qquad for\ j = 0,1,2,\ldots,m, s \in \Omega, \\ \left(1 - \frac{\Delta t}{2}\mathcal{L}_\varepsilon{}^{\Delta t}\right)Z^j(s) - \Delta t\mu(s,t_{j+1/2})Z^{j+1/2-m}(s) \\ +\Delta t f(s,t_{j+1/2}), \qquad for\ j = m+1,\ldots,M-1, s \in \Omega, \\ Z^{j+1}(0) = \psi_l(t_{j+1}), \qquad Z^{j+1}(1) = \psi_r(t_{j+1}),\ \ 0 \leq j \leq M, \end{cases} \tag{8}$$

where ${\mathcal{L}_\varepsilon}^{\Delta t} Z^{j+1}(s) = -\varepsilon \frac{d^2 Z^{j+1}(s)}{ds^2} + \kappa(s)\frac{dZ^{j+1}(s)}{ds} + \gamma(s,t_{j+1})Z^{j+1}(s)$ and $Z(s) = Z^{j+1}(s) \approx z(s,t_{j+1})$. The local error is defined as $e_{j+1}(s) = z(s,t_{j+1}) - Z^{j+1}(s),\ j = 0(1)M$.

Lemma 6. The local error estimate at t_{j+1} is given as

$$\|e_{j+1}\| \leq C(\Delta t)^3, \tag{9}$$

and the global error bound at $j+1$th time level is given as

$$\|E_{j+1}\| \leq C(\Delta t)^2, \qquad j = 1(1)M-1. \tag{10}$$

Proof. From the local error estimate, it follows that

$$\begin{aligned} \|E_{j+1}\| =& \left\| \sum_{l=1}^{j+1} e_l \right\| \leq \|e_1\| + \|e_2\| + \|e_3\| + \cdots + \|e_{j+1}\| \\ \leq& C_1 \mathbb{T}(\Delta t)^2 \qquad \text{since} \quad (j+1)\Delta t \leq \mathbb{T}, \\ =& C(\Delta t)^2, \qquad \text{where} \qquad C_1\mathbb{T} = C, \end{aligned}$$

where C is constant independent of ε and Δt. □

Lemma 7. For $j = 0(1)M-1$, $p = 0(1)4$, then the derivative of the solution of (7) satisfies the estimate

$$\left| \frac{d^p Z^{j+1}(s)}{ds^p} \right| \leq C\left(1 + \varepsilon^{-p} \exp\left(-\frac{\beta}{\varepsilon}(1-s)\right)\right), \quad s \in \bar{\Omega}. \tag{11}$$

Proof. For the proof see [10]. □

3.2 Spatial discretization

The spatial domain $[0,1]$ into N equal number of sub-intervals with the length of h is given by $0 = s_0, s_1, \ldots, s_N = 1$ and $s_i = ih,\ i = 0(1)N$.

3.2.1 Description of the method

A function $\mathfrak{S}(s,\tau)$ in $C(\bar{\Omega})$ interpolates $z(s)$ at the mesh points s_i that depends on the compression parameter τ and reduces to a cubic spline on $\bar{\Omega}$ as

$\tau \to 0$ is referred as a parametric cubic spline function [11]. For each interval $[s_i, s_{i+1}]$, $i = 1(1)N-1$ the spline function $\mathfrak{S}(s,\tau) = \mathfrak{S}(s)$ has the form

$$\mathfrak{S}_{ss}(s,t_{j+1}) - \tau\mathfrak{S}(s,t_{j+1}) = [\mathfrak{S}_{ss}(s_i,t_{j+1}) - \tau\mathfrak{S}(s_i,t_{j+1})]\frac{s_{i+1}-s}{h} + [\mathfrak{S}_{ss}(s_{i+1},t_{j+1}) - \tau\mathfrak{S}(s_{i+1},t_{j+1})]\frac{s-s_i}{h}, \quad (12)$$

where $\mathfrak{S}(s_i,t_{j+1}) = Z_i^{j+1}$ for $\tau > 0$ is called cubic spline in tension [5]. Putting $\sqrt{\tau} = \frac{\alpha}{h}$ and from the homogeneous part of (12), we get

$$\mathfrak{S}_1(s,t_{j+1}) = \mathfrak{A}e^{\frac{\alpha}{h}(s-s_i)} + \mathfrak{B}e^{\frac{\alpha}{h}(s_{i+1}-s)}, \quad (13)$$

for arbitrary constants $\mathfrak{A}$ and $\mathfrak{B}$. Let the nonhomogeneous part be given as

$$\mathfrak{S}_2(s,t_{j+1}) = -1/\tau\Big([\mathfrak{S}_{ss}(s_i,t_{j+1}) - \tau\mathfrak{S}(s_i,t_{j+1})]\frac{s_{i+1}-s}{h} + [\mathfrak{S}_{ss}(s_{i+1},t_{j+1}) - \tau\mathfrak{S}(s_{i+1},t_{j+1})]\frac{s-s_i}{h}\Big). \quad (14)$$

Thus, we have

$$\mathfrak{S}_2(s,t_{j+1}) = -\left(\frac{h}{\alpha}\right)^2[\mathfrak{M}_i - \left(\frac{\alpha}{h}\right)^2 Z_i^{j+1}]\frac{s_{i+1}-s}{h} - \left(\frac{h}{\alpha}\right)^2[\mathfrak{M}_{i+1} - \left(\frac{\alpha}{h}\right)^2 Z_{i+1}^{j+1}]\frac{s-s_i}{h}, \quad (15)$$

where $\mathfrak{M}_i = \mathfrak{S}_{ss}(s_i,t_{j+1})$ and $\mathfrak{M}_{i+1} = \mathfrak{S}_{ss}(s_{i+1},t_{j+1})$. Using (13) and (15), we get

$$\mathfrak{S}(s,t_{j+1}) = \mathfrak{A}e^{\frac{\alpha}{h}(s-s_i)} + \mathfrak{B}e^{\frac{\alpha}{h}(s_{i+1}-s)} - \left(\frac{h}{\alpha}\right)^2[\mathfrak{M}_i - \left(\frac{\alpha}{h}\right)^2 Z_i^{j+1}]\frac{s_{i+1}-s}{h} - \left(\frac{h}{\alpha}\right)^2[\mathfrak{M}_{i+1} - \left(\frac{\alpha}{h}\right)^2 Z_{i+1}^{j+1}]\frac{s-s_i}{h}. \quad (16)$$

From (16), the arbitrary constants can be determined from the interpolation conditions $\mathfrak{S}(s_i,t_{j+1})$ and $\mathfrak{S}(s_{i+1},t_{j+1})$. Then

$$\mathfrak{S}(s,t_{j+1}) = \frac{h^2}{\alpha^2\sinh\alpha}\left[\mathfrak{M}_{i+1}\sinh\left(\frac{\alpha(s-s_i)}{h}\right) + \mathfrak{M}_i\sinh\left(\frac{\alpha(s_{i+1}-s)}{h}\right)\right] - \left[\frac{h}{\alpha^2}\mathfrak{M}_i - \frac{1}{h}Z_i^{j+1}\right](s_{i+1}-s) - \left[\frac{h}{\alpha^2}\mathfrak{M}_{i+1} - \frac{1}{h}Z_{i+1}^{j+1}\right](s-s_i). \quad (17)$$

The derivative of (17) at (s_i, t_{j+1}) on the interval $[s_i, s_{i+1}]$ is

$$\mathfrak{S}(s_i^+, t_{j+1}) = \frac{Z_{i+1}^{j+1} - Z_i^{j+1}}{h} - \frac{h}{\alpha^2}[\mathfrak{M}_{i+1}(1-\alpha csch\alpha) + \mathfrak{M}_i(\alpha \coth \alpha - 1)], \quad (18)$$

and on the interval $[s_{i-1}, s_i]$ is

$$\mathfrak{S}(s_i^-, t_{j+1}) = \frac{Z_i^{j+1} - Z_{i-1}^{j+1}}{h} + \frac{h}{\alpha^2}[\mathfrak{M}_i(\alpha \coth \alpha - 1) + \mathfrak{M}_{i-1}(1-\alpha csch\alpha)]. \quad (19)$$

Equating (18) and (19) at the point s_i, we get

$$\begin{aligned}\frac{Z_{i-1}^{j+1} - 2Z_i^{j+1} + Z_{i+1}^{j+1}}{h^2} =& \frac{\mathfrak{M}_{i-1}(1-\alpha csch\alpha)}{\alpha^2} + \frac{2\mathfrak{M}_i(\alpha \coth \alpha - 1)}{\alpha^2} \\ &+ \frac{\mathfrak{M}_{i+1}(1-\alpha csch\alpha)}{\alpha^2}.\end{aligned} \quad (20)$$

Simplifying we obtain

$$\frac{Z_{i-1}^{j+1} - 2Z_i^{j+1} + Z_{i+1}^{j+1}}{h^2} = \alpha_1 \mathfrak{M}_{i-1} + 2\alpha_2 \mathfrak{M}_i + \alpha_1 \mathfrak{M}_{i+1}, \qquad i = 1(1)N-1, \quad (21)$$

where $\alpha_1 = \alpha^{-2}(1 - \alpha csch\alpha)$ and $\alpha_2 = \alpha^{-2}(\alpha \coth \alpha - 1)$. The continuity condition in (21) ensures the continuity of the first derivative of $\mathfrak{S}(s)$ at interior nodes. From (7), at the grid point $j+1$ we determine $Z_i^{''} = \mathfrak{M}_i = \mathfrak{S}_{ss}(s_i, t_{j+1})$ as

$$\begin{cases} -\varepsilon \mathfrak{M}_i = \quad -\kappa(s_i)Z_i^{'} - \gamma(s_i, t_{j+1})Z_i + \mathfrak{R}(s_i, t_{j+1}), \\ -\varepsilon \mathfrak{M}_{i\pm1} = -\kappa(s_{i\pm1})Z_{i\pm1}^{'} - \gamma(s_{i\pm1}, t_{j+1})Z_{i\pm1} + \mathfrak{R}(s_{i\pm1}, t_{j+1}), \end{cases} \quad (22)$$

where

$$\mathfrak{R}(s_i, t_{j+1}) = \begin{cases} -0.5\Delta t \mu(s_i, t_{j+1})\psi_b(s_i) + 0.5\Delta t f(s_i, t_{j+1}), \\ \qquad for\ j = 0, 1, 2, \ldots, m, s \in \Omega, \\ -0.5\Delta t \mu(s_i, t_{j+1}) Z_i^{j+1-m} + 0.5\Delta t f(s_i, t_{j+1}), \\ \qquad for\ j = m+1, \ldots, M-1, s \in \Omega, \\ Z^{j+1}(0) = \psi_l(t_{j+1}), \ \ Z^{j+1}(1) = \psi_r(t_{j+1}), \ \ 0 \le j \le M. \end{cases} \quad (23)$$

The local truncation error $\mathfrak{T}_1(h)$ obtained from (21) is

$$\mathfrak{T}_1(h) = \frac{h^4}{3}(-2\alpha_1 + \alpha_2)\kappa(s_i)Z^{'''}(s_i) + \frac{h^4}{12}(1 - 12\alpha_1)\kappa(s_i)\varepsilon Z^{(4)}(s_i) + O(h^6), \quad (24)$$

for any choice of α_1 and α_2 whose sum is 1/2. For the choice $\alpha_1 = 1/12$ and $\alpha_2 = 5/12$, we have

$$\mathfrak{T}_1(h) = \frac{\varepsilon h^6}{240} Z^{(6)}(s_i), \qquad s_i \in [s_{i-1}, s_{i+1}]. \tag{25}$$

We approximate $Z'_{i\pm1}$ and Z'_i as

$$\begin{cases} Z'_i \approx \frac{Z_{i+1}-Z_{i-1}}{2h}, \\ Z'_{i+1} \approx \frac{3Z_{i+1}-4Z_i+Z_{i-1}}{2h}, \\ Z'_{i-1} \approx \frac{-Z_{i+1}+4Z_i-3Z_{i-1}}{2h}. \end{cases} \tag{26}$$

Substituting (26) and (22) into (21) and rearranging, we get

$$\begin{aligned}(1+\frac{\Delta t}{2}{\mathcal{L}_\varepsilon}^{\Delta t,h})Z_i^{j+1} =&(1-\frac{\Delta t}{2}{\mathcal{L}_\varepsilon}^{\Delta t,h})Z_i^j + \alpha_1(\mathfrak{R}(s_{i-1},t_j)+\mathfrak{R}(s_{i-1},t_{j+1})) \\ &+ 2\alpha_2(\mathfrak{R}(s_i,t_j)+\mathfrak{R}(s_i,t_{j+1})) + \alpha_1(\mathfrak{R}(s_{i+1},t_j) \\ &+ \mathfrak{R}(s_{i+1},t_{j+1})),\end{aligned} \tag{27}$$

where

$$\begin{aligned}(1+\frac{\Delta t}{2}{\mathcal{L}_\varepsilon}^{\Delta t,h})Z_i^{j+1} \equiv& \frac{-\varepsilon\Delta t}{2h^2}(Z_{i-1}^{j+1}-2Z_i^{j+1}+Z_{i+1}^{j+1}) + \frac{\alpha_1\Delta t\kappa(s_{i-1})}{4h}(-3Z_{i-1}^{j+1} \\ &+ 4Z_i^{j+1} - Z_{i+1}^{j+1}) + \frac{\alpha_2\Delta t\kappa(s_i)}{2h}(Z_{i+1}^{j+1}-Z_{i-1}^{j+1}) \\ &+ \frac{\alpha_1\Delta t\kappa(s_{i+1})}{4h}(Z_{i-1}^{j+1}-4Z_i^{j+1}+3Z_{i+1}^{j+1}) \\ &+ \alpha_1(1+0.5\Delta t\gamma(s_{i-1},t_{j+1}))Z_{i-1}^{j+1} \\ &+ \alpha_2(2+\Delta t\gamma(s_i,t_{j+1}))Z_i^{j+1} \\ &+ \alpha_1(1+0.5\Delta t\gamma(s_{i+1},t_{j+1}))Z_{i+1}^{j+1}.\end{aligned} \tag{28}$$

To handle the steep gradient of the solution, we introduce the exponential fitting factor σ. Now, multiplying term containing ε of (28) by σ, we obtain

$$\begin{aligned}
&\frac{-\sigma\varepsilon\Delta t}{2h^2}(Z_{i-1}^{j+1}-2Z_i^{j+1}+Z_{i+1}^{j+1})+\frac{\alpha_1\Delta t\kappa(s_{i-1})}{4h}(-3Z_{i-1}^{j+1}+4Z_i^{j+1}-Z_{i+1}^{j+1})\\
&+\frac{\alpha_2\Delta t\kappa(s_i)}{2h}(Z_{i+1}^{j+1}-Z_{i-1}^{j+1})+\frac{\alpha_1\Delta t\kappa(s_{i+1})}{4h}(Z_{i-1}^{j+1}-4Z_i^{j+1}+3Z_{i+1}^{j+1})\\
&+\alpha_1(1+0.5\Delta t\gamma(s_{i+1},t_{j+1}))Z_{i-1}^{j+1}+\alpha_2(2+\Delta t\gamma(s_{i+1},t_{j+1}))Z_i^{j+1}\\
&+\alpha_1(1+0.5\Delta t\gamma(s_{i+1},t_{j+1}))Z_{i+1}^{j+1}=\alpha_1\Re(s_{i-1},t_{j+1})+2\alpha_2\Re(s_i,t_{j+1})\\
&\qquad\qquad+\alpha_1\Re(s_{i+1},t_{j+1}).
\end{aligned} \tag{29}$$

From [18], the zero-order asymptotic solution of problem (7) about $s=1$ is given as

$$Z(s_i)=Z(ih)\approx Z_0(1)+(\psi_r-Z_0(1))\exp(-\kappa(1)i\rho), \tag{30}$$

where $\rho=\frac{h}{\varepsilon}$. Multiplying (29) by h and taking a limit as $h\to 0$, which gives

$$\begin{aligned}
&-\frac{\sigma}{\rho}\lim_{h\to 0}(Z_{i-1}-2Z_i+Z_{i+1})+\frac{\alpha_1\kappa(1)}{2}\lim_{h\to 0}(-3Z_{i-1}+4Z_i-Z_{i+1})\\
&+\alpha_2\kappa(1)\lim_{h\to 0}(Z_{i+1}-Z_{i-1})+\frac{\alpha_1\kappa(1)}{2}\lim_{h\to 0}(Z_{i-1}-4Z_i+3Z_{i+1})=0,
\end{aligned} \tag{31}$$

$$\begin{cases}
\lim_{h\to 0}(Z((i-1)h)-2Z(ih)+Z((i+1)h))\\
\qquad=(\psi_r-Z_0(1))e^{(-\kappa(1)i\rho)}(e^{\kappa(1)\rho}+e^{-\kappa(1)\rho}-2),\\
\lim_{h\to 0}(-3Z((i-1)h)+4Z(ih)-Z((i+1)h))\\
\qquad=(\psi_r-Z_0(1))e^{(-\kappa(1)i\rho)}(-3e^{\kappa(1)\rho}-e^{-\kappa(1)\rho}+4),\\
\lim_{h\to 0}(Z((i-1)h)-4Z(ih)+3Z((i+1)h))\\
\qquad=(\psi_r-Z_0(1))e^{(-\kappa(1)i\rho)}(e^{\kappa(1)\rho}+3e^{-\kappa(1)\rho}-4),\\
\lim_{h\to 0}(Z((i+1)h)-Z((i-1)h))\\
\qquad=(\psi_r-Z_0(1))e^{(-\kappa(1)i\rho)}(e^{-\kappa(1)\rho}-e^{\kappa(1)\rho}).
\end{cases} \tag{32}$$

Substituting (32) into (31), we obtain

$$\sigma=\rho\kappa(1)(\alpha_1+\alpha_2)\coth(\frac{\rho\kappa(1)}{2}). \tag{33}$$

The variable exponential fitting factor is given as

$$\sigma_i=\rho\kappa(s_i)(\alpha_1+\alpha_2)\coth(\frac{\rho\kappa(s_i)}{2}). \tag{34}$$

Using (34) and (27) for $i=1(1)N-1$ and $j=1(1)M-1$, we have

$$
\begin{aligned}
(1+\frac{\Delta t}{2}{\mathcal{L}_{\varepsilon}}^{\Delta t,h})Z_i^{j+1} =&(1-\frac{\Delta t}{2}{\mathcal{L}_{\varepsilon}}^{\Delta t,h})Z_i^{j}+\alpha_1(\Re(s_{i-1},t_j)+\Re(s_{i-1},t_{j+1}))\\
&+2\alpha_2(\Re(s_i,t_j)+\Re(s_i,t_{j+1}))\\
&+\alpha_1(\Re(s_{i+1},t_j)+\Re(s_{i+1},t_{j+1})),
\end{aligned}
\tag{35}
$$

where

$$
\begin{aligned}
(1+\frac{\Delta t}{2}{\mathcal{L}_{\varepsilon}}^{\Delta t,h})Z_i^{j+1} \equiv&\frac{-\varepsilon\sigma_i\Delta t}{2h^2}(Z_{i-1}^{j+1}-2Z_i^{j+1}+Z_{i+1}^{j+1})\\
&+\frac{\alpha_1\Delta t\kappa(s_{i-1})}{4h}(-3Z_{i-1}^{j+1}+4Z_i^{j+1}-Z_{i+1}^{j+1})\\
&+\frac{\alpha_2\Delta t\kappa(s_i)}{2h}(Z_{i+1}^{j+1}-Z_{i-1}^{j+1})\\
&+\frac{\alpha_1\Delta t\kappa(s_{i+1})}{4h}(Z_{i-1}^{j+1}-4Z_i^{j+1}+3Z_{i+1}^{j+1})\\
&+\alpha_1(1+0.5\Delta t\gamma(s_{i-1},t_{j+1}))Z_{i-1}^{j+1}\\
&+\alpha_2(2+\Delta t\gamma(s_i,t_{j+1}))Z_i^{j+1}\\
&+\alpha_1(1+0.5\Delta t\gamma(s_{i+1},t_{j+1}))Z_{i+1}^{j+1}.
\end{aligned}
\tag{36}
$$

Finally, (35) can be written as a system of equation

$$
\begin{aligned}
\mathfrak{D}_i^-Z_{i-1}^{j+1}+\mathfrak{D}_i^0Z_i^{j+1}+\mathfrak{D}_i^+Z_{i+1}^{j+1} =&\mathfrak{E}_i^-Z_{i-1}^{j}+\mathfrak{E}_i^0Z_i^{j}+\mathfrak{E}_i^+Z_{i+1}^{j}\\
&+\alpha_1(\Re(s_{i-1},t_j)+\Re(s_{i-1},t_{j+1}))\\
&+2\alpha_2(\Re(s_i,t_j)+\Re(s_i,t_{j+1}))\\
&+\alpha_1(\Re(s_{i+1},t_j)+\Re(s_{i+1},t_{j+1})),
\end{aligned}
\tag{37}
$$

where

$$
\begin{cases}
\mathfrak{D}_i^- = -\frac{\varepsilon\sigma_i}{2h^2}-\frac{3\alpha_1\kappa(s_{i-1})}{4h}-\frac{\alpha_2\kappa(s_i)}{2h}+\frac{\alpha_1\kappa(s_{i+1})}{4h}+0.5\alpha_1\gamma(s_{i-1},t_{j+1})+\frac{\alpha_1}{\Delta t},\\
\mathfrak{D}_i^0 = \frac{\varepsilon\sigma_i}{h^2}+\frac{\alpha_1\kappa(s_{i-1})}{h}-\frac{\alpha_1\kappa(s_{i+1})}{h}+\alpha_2\gamma(s_i,t_{j+1})+\frac{2\alpha_2}{\Delta t},\\
\mathfrak{D}_i^+ = -\frac{\varepsilon\sigma_i}{2h^2}-\frac{\alpha_1\kappa(s_{i-1})}{4h}+\frac{\alpha_2\kappa(s_i)}{2h}+\frac{3\alpha_1\kappa(s_{i+1})}{4h}+0.5\alpha_1\gamma(s_{i+1},t_{j+1})+\frac{\alpha_1}{\Delta t},
\end{cases}
\tag{38}
$$

$$
\begin{cases}
\mathfrak{E}_i^- = \frac{\varepsilon\sigma_i}{2h^2}+\frac{3\alpha_1\kappa(s_{i-1})}{4h}+\frac{\alpha_2\kappa(s_i)}{2h}-\frac{\alpha_1\kappa(s_{i+1})}{4h}-0.5\alpha_1\gamma(s_{i-1},t_{j+1})+\frac{\alpha_1}{\Delta t},\\
\mathfrak{E}_i^0 = -\frac{\varepsilon\sigma_i}{h^2}-\frac{\alpha_1\kappa(s_{i-1})}{h}+\frac{\alpha_1\kappa(s_{i+1})}{h}-\alpha_2\gamma(s_i,t_j)+\frac{2\alpha_2}{\Delta t},\\
\mathfrak{E}_i^+ = \frac{\varepsilon\sigma_i}{2h^2}+\frac{\alpha_1\kappa(s_{i-1})}{4h}-\frac{\alpha_2\kappa(s_i)}{2h}-\frac{3\alpha_1\kappa(s_{i+1})}{4h}-0.5\alpha_1\gamma(s_{i+1},t_j)+\frac{\alpha_1}{\Delta t},
\end{cases}
\tag{39}
$$

$$\Re(s_i,t_{j+1}) = \begin{cases} -0.5\mu(s_i,t_{j+1})\psi_b(s_i) + 0.5f(s_i,t_{j+1}), \\ \qquad\qquad for\ j=0,1,2,\ldots,m, s\in\Omega, \\ -0.5\Delta t\mu(s_i,t_{j+1})Z_i^{j+1-m} + 0.5f(s_i,t_{j+1}), \\ \qquad\qquad for\ j=m+1,\ldots,M-1, s\in\Omega, \quad 0\le j\le M. \end{cases} \tag{40}$$

3.3 Convergence analysis

Lemma 8 (Discrete maximum principle)**.** Assume that $Z_0^{j+1}\ge 0, Z_N^{j+1}\ge 0$ and $(1+\frac{\Delta t}{2}\mathcal{L}_\varepsilon{}^{\Delta t,h})Z_i^{j+1} \ge 0$, for all $i = 1(1)N-1$; then $Z_i^{j+1} \ge 0$, for all $i=0(1)N$.

Proof. Assume there is $k\in\{0,1,2,\ldots,N\}$ such that $Z_k^{j+1} = \min_{0\le i\le N} Z_i^{j+1} < 0$. Assume that $Z_k^{j+1}<0$ and from the assumption, it is shown that $k\notin\{0,1\}$. So that, we have $Z_{k+1}^{j+1}-Z_k^{j+1}>0$ and $Z_k^{j+1}-Z_{k-1}^{j+1}<0$. Then, we get $(1+\frac{\Delta t}{2}\mathcal{L}_\varepsilon{}^{\Delta t,h})Z_i^{j+1}<0$ for $k=1(1)N-1$. So, the assumption $Z_i^{j+1}<0$ for all $i=0(1)N$ is wrong. Therefore, $Z_i^{j+1}\ge 0$, for all $i=0(1)N$. □

Lemma 9 (Stability result)**.** The solution Z_i^{j+1} of the scheme in (35) satisfies

$$\left|Z_i^{j+1}\right| \le \frac{\|\ (1+\frac{\Delta t}{2}\mathcal{L}_\varepsilon{}^{\Delta t,h})Z_i^{j+1}\|}{1+\frac{\delta t}{2}\varpi} + \max\{|\psi_l(t_{j+1})|,|\psi_r(t_{j+1})|\}.$$

Proof. Let $\Pi = \frac{\|\ (1+\frac{\Delta t}{2}\mathcal{L}_\varepsilon{}^{\Delta t,h})Z_i^{j+1}\|}{1+\frac{\Delta t}{2}\varpi} + \max\{|\psi_l(t_{j+1})|,|\psi_r(t_{j+1})|\}$, and set the barrier functions $\vartheta_{i,j+1}^{\pm}$ as $\vartheta_{i,j+1}^{\pm} = \Pi \pm Z_i^{j+1}$. On the boundaries, we have

$$\begin{aligned}\vartheta_{0,j+1}^{\pm} &= \Pi \pm Z_0^{j+1} \\ &= \frac{\|\ (1+\frac{\Delta t}{2}\mathcal{L}_\varepsilon{}^{\Delta t,h})Z_i^{j+1}\|}{1+\frac{\Delta t}{2}\varpi} + \max\{|\psi_l(t_{j+1})|,|\psi_r(t_{j+1})|\} \pm \psi_l(t_{j+1}) \\ &\ge 0,\end{aligned}$$

and

$$\begin{aligned}\vartheta_{N,j+1}^{\pm} &= \Pi \pm Z_N^{j+1} \\ &= \frac{\|\ (1+\frac{\Delta t}{2}\mathcal{L}_\varepsilon{}^{\Delta t,h})Z_i^{j+1}\|}{1+\frac{\Delta t}{2}\varpi} + \max\{|\psi_l(t_{j+1})|,|\psi_r(t_{j+1})|\} \pm \psi_r(t_{j+1})\end{aligned}$$

$\geq 0.$

On the discretized domain $s_i,\ i=1(1)N-1$, we have

$$
\begin{aligned}
\left(1+\frac{\Delta t}{2}{\mathcal{L}_\varepsilon}^{\Delta t,h}\right)\vartheta^{\pm}_{i,j+1} =&\Pi \pm Z_i^{j+1} - (\varepsilon\sigma_i)\frac{\Delta t}{2h^2}\Big(\Pi \pm Z_{i-1}^{j+1} - 2(\Pi \pm Z_i^{j+1}) \\
&+ \Pi \pm Z_{i+1}^{j+1}\Big) + \alpha_1\Delta t\frac{\kappa(s_{i-1})}{4h}\Big(-3(\Pi \pm Z_{i-1}^{j+1}) \\
&+ 4(\Pi \pm Z_i^{j+1}) - (\Pi \pm Z_{i+1}^{j+1})\Big) \\
&+ \alpha_2\Delta t\frac{\kappa(s_i)}{2h}\Big(\Pi \pm Z_{i+1}^{j+1} - (\Pi \pm Z_{i-1}^{j+1})\Big) \\
&+ \alpha_1\Delta t\frac{\kappa(s_{i+1})}{4h}\Big(\Pi \pm Z_{i-1}^{j+1} - 4(\Pi \pm Z_i^{j+1}) \\
&+ 3(\Pi \pm Z_{i+1}^{j+1})\Big) + \frac{\Delta t}{2}\alpha_1\gamma(s_{i-1},t_{j+1})\big(\Pi \pm Z_{i-1}^{j+1}\big) \\
&+ \Delta t\alpha_2\gamma(s_i,t_{j+1})\big(\Pi \pm Z_i^{j+1}\big) \\
&+ \frac{\Delta t}{2}\alpha_1\gamma(s_{i+1},t_{j+1})\big(\Pi \pm Z_{i+1}^{j+1}\big) \\
=&\big(1+\frac{\Delta t}{2}\alpha_1\gamma(s_{i-1},t_{j+1}) + \Delta t\alpha_2\gamma(s_i,t_{j+1}) \\
&+ \frac{\Delta t}{2}\alpha_1\gamma(s_{i+1},t_{j+1})\big)\Pi \pm \left(1+\frac{\Delta t}{2}{\mathcal{L}_\varepsilon}^{\Delta t,h}\right)Z_i^{j+1} \\
=&\big(1+\frac{\Delta t}{2}\alpha_1\gamma(s_{i-1},t_{j+1}) + \Delta t\alpha_2\gamma(s_i,t_{j+1}) \\
&+ \frac{\Delta t}{2}\alpha_1\gamma(s_{i+1},t_{j+1})\big)\left(\frac{\| (1+\frac{\Delta t}{2}{\mathcal{L}_\varepsilon}^{\Delta t,h})Z_i^{j+1}\|}{1+\frac{\Delta t}{2}\varpi}\right. \\
&\left.+ \max\{|\psi_l(t_{j+1})|, |\psi_r(t_{j+1})|\}\right) \\
&\pm \left(1+\frac{\Delta t}{2}{\mathcal{L}_\varepsilon}^{\Delta t,h}\right)Z_i^{j+1} \geq 0.
\end{aligned}
\tag{41}
$$

From Lemma 8, we get $\vartheta^{\pm}_{i,j+1} \geq 0,\ i=0(1)N$. Hence, the necessary bound is satisfied. □

Using Taylor's series approximation, we have the bounds

$$
\begin{aligned}
\left| -\left(\frac{d}{ds^2} - \delta_s^2\right) Z^{j+1}(s_i) \right| \leq & Ch^2 \left\| \frac{d^4 Z^{j+1}(s_i)}{ds^4} \right\|, \\
\left| \frac{dZ^{j+1}(s_{i-1})}{ds} - \left(\frac{-Z_{i+1}^{j+1} + 4Z_i^{j+1} - 3Z_{i-1}^{j+1}}{2h} \right) \right| \leq & Ch^2 \left\| \frac{d^3 Z^{j+1}(s_i)}{ds^3} \right\|, \\
\left| \frac{dZ^{j+1}(s_{i+1})}{ds} - \left(\frac{3Z_{i+1}^{j+1} - 4Z_i^{j+1} + Z_{i-1}^{j+1}}{2h} \right) \right| \leq & Ch^2 \left\| \frac{d^3 Z^{j+1}(s_i)}{ds^3} \right\|, \\
\left| \left(\frac{d}{ds} - \delta_s^0\right) Z^{j+1}(s_i) \right| \leq Ch^2 \left\| \frac{d^3 Z^{j+1}(s_i)}{ds^3} \right\|, \left| \delta_s^2 Z^{j+1}(s_i) \right| \leq & C \left\| \frac{d^2 Z^{j+1}(s_i)}{ds^2} \right\|,
\end{aligned}
\tag{42}
$$

where $\|Z_{j+1}^{(p)}(s_i)\| = \max_{s_0 \leq s_i \leq s_N} |Z_{j+1}^{(p)}(s_i)|$, $p = 2, 3, 4$.

For the constants $\rho > 0,\ C_1$ and C_2, we have

$$
C_1 \frac{\rho^2}{\rho + 1} \leq \rho \coth(\rho) - 1 \leq C_2 \frac{\rho^2}{\rho + 1}. \tag{43}
$$

Following (43), we have

$$
\begin{aligned}
\left| \varepsilon[\rho\kappa(1)(\alpha_1 + \alpha_2) \coth(\frac{\rho\kappa(1)}{2}) - 1] \delta_s^2 Z^{j+1}(s_i) \right| \leq & \varepsilon \frac{C(h/\varepsilon)^2}{h/\varepsilon + 1} \left\| \frac{d^2 Z^{j+1}(s_i)}{ds^2} \right\| \\
= & \frac{Ch^2}{h + \varepsilon} \left\| \frac{d^2 Z^{j+1}(s_i)}{ds^2} \right\|,
\end{aligned}
\tag{44}
$$

since $\alpha_1 + \alpha_2 \leq 1/2$.

The next theorem provides the error bound in the space direction for the boundary layer along $s = 1$.

Theorem 1. Let $Z^{j+1}(s)$ be the solution of (7). Then the solution Z_i^{j+1} of (35) satisfies the following error estimate

$$
\left| \mathcal{L}_\varepsilon{}^{\Delta t, h} (Z^{j+1}(s_i) - Z_i^{j+1}) \right| \leq \frac{Ch^2}{h + \varepsilon} \left(1 + \varepsilon^{-3} \exp\left(-\frac{\beta}{\varepsilon}(1 - s_i) \right) \right). \tag{45}
$$

Proof. In the spatial direction, the local truncation error is given by

$$
\begin{aligned}
\left|\mathcal{L}_{\varepsilon}{}^{\Delta t,h}(Z^{j+1}(s_i)-Z_i^{j+1})\right| \leq & \Bigg| -\varepsilon\left(\frac{d}{ds^2}-\sigma_i\delta_s^2\right)Z^{j+1}(s_i) \\
& +\alpha_1\kappa(s_{i-1})\Bigg(\frac{dZ^{j+1}(s_{i-1})}{ds} \\
& -\left(\frac{-3Z_{i-1}^{j+1}+4Z_i^{j+1}-Z_{i+1}^{j+1}}{2h}\right)\Bigg) \\
& +2\alpha_2\kappa(s_i)\left(\frac{d}{ds}-\delta_s^0\right)Z^{j+1}(s_i) \\
& +\alpha_1\kappa(s_{i+1})\Bigg(\frac{dZ^{j+1}(s_{i+1})}{ds} \\
& -\left(\frac{Z_{i-1}^{j+1}-4Z_i^{j+1}+3Z_{i+1}^{j+1}}{2h}\right)\Bigg)\Bigg| + \left|\mathfrak{T}_1(h)\right| \\
\leq & \left|\varepsilon[\rho\kappa(1)(\alpha_1+\alpha_2)\coth(\kappa(1)\frac{\rho}{2})-1]\delta_s^2 Z^{j+1}(s_i))\right| \\
& +\left|\varepsilon\left(\frac{d^2}{ds^2}-\delta_s^2\right)Z^{j+1}(s_i)\right| \\
& +\Bigg|\alpha_1\kappa(s_{i-1})\Bigg(\frac{dZ^{j+1}(s_{i-1})}{ds} \\
& -\left(\frac{-3Z_{i-1}^{j+1}+4Z_i^{j+1}-Z_{i+1}^{j+1}}{2h}\right)\Bigg)\Bigg| \\
& +\left|2\alpha_2\kappa(s_i)\left(\frac{d}{ds}-\delta_s^0\right)Z^{j+1}(s_i)\right| \\
& +\Bigg|\alpha_1\kappa(s_{i+1})\Bigg(\frac{dZ^{j+1}(s_{i+1})}{ds} \\
& -\left(\frac{Z_{i-1}^{j+1}-4Z_i^{j+1}+3Z_{i+1}^{j+1}}{2h}\right)\Bigg)\Bigg| + \left|\mathfrak{T}_1(h)\right|.
\end{aligned}
$$

Using the bounds in (42) and (44), we obtain

$$
\begin{aligned}
\left|\mathcal{L}_{\varepsilon}{}^{\Delta t,h}(Z^{j+1}(s_i)-Z_i^{j+1})\right| \leq & \frac{Ch^2}{h+\varepsilon}\left\|\frac{d^2Z^{j+1}(s_i)}{ds^2}\right\| \\
& +Ch^2\left\|\frac{d^3Z^{j+1}(s_i)}{ds^3}\right\| + C\varepsilon h^2\left\|\frac{d^4Z^{j+1}(s_i)}{ds^4}\right\| \\
& +Ch^4(-2\alpha_1+\alpha_2)\left\|\frac{d^3Z^{j+1}(s_i)}{ds^3}\right\| \\
& +C\varepsilon h^4(1-12\alpha_1)\left\|\frac{d^4Z^{j+1}(s_i)}{ds^4}\right\|.
\end{aligned}
$$

From Lemma 7, we obtain

$$
\begin{aligned}
\left|\mathcal{L}_{\varepsilon}{}^{\Delta t,h}(Z^{j+1}(s_i) - Z_i^{j+1})\right| \leq & \frac{Ch^2}{h+\varepsilon}\left(1+\varepsilon^{-2}\exp\left(-\frac{\beta}{\varepsilon}(1-s_i)\right)\right) \\
& + Ch^2\left[1+\varepsilon^{-3}\exp\left(-\frac{\beta}{\varepsilon}(1-s_i)\right)\right. \\
& \left. + \varepsilon + \varepsilon^{-3}\exp\left(-\frac{\beta}{\varepsilon}(1-s_i)\right)\right] \\
& + Ch^4(-2\alpha_1+\alpha_2)\left(1+\varepsilon^{-3}\exp\left(-\frac{\beta}{\varepsilon}(1-s_i)\right)\right) \\
& + Ch^4(1-12\alpha_1)\left(\varepsilon+\varepsilon^{-3}\exp\left(-\frac{\beta}{\varepsilon}(1-s_i)\right)\right) \\
\leq & \frac{Ch^2}{h+\varepsilon}\left(1+\varepsilon^{-3}\exp\left(-\frac{\beta}{\varepsilon}\left(1-s_i\right)\right)\right),
\end{aligned}
$$

since $\varepsilon^{-2} \leq \varepsilon^{-3}$ and obtain the desired bound. □

Lemma 10. For a fixed mesh and as $\varepsilon \to 0$, it gives

$$
\lim_{\varepsilon\to 0}\max_i \frac{\exp(-\beta s_i/\varepsilon)}{\varepsilon^p} = 0, \qquad \lim_{\varepsilon\to 0}\max_i \frac{\exp(-\beta(1-s_i)/\varepsilon)}{\varepsilon^p} = 0, \tag{46}
$$

where $p = 1, 2, 3, \ldots,\ \ s_i = ih,\ i = 1(1)N-1$.

Proof. The proof can be done by using L'Hospital's rule. For details, refer to [27]. □

Theorem 2. Let Z_i^{j+1} be the solution of (35). Then we have the following uniform error bound:

$$
\sup_{\varepsilon\in(0,1]}\max_i \left|Z^{j+1}(s_i) - Z_i^{j+1}\right| \leq Ch,\ i = 0(1)N. \tag{47}
$$

Proof. Substituting Lemma 10 into (45), we arrive at

$$
\left|\mathcal{L}^{\Delta t,h}(Z^{j+1}(s_i) - Z_i^{j+1})\right| \leq \frac{Ch^2}{h+\varepsilon}. \tag{48}
$$

Hence, the result leads $\left|Z^{j+1}(s_i) - Z_i^{j+1}\right| \leq \frac{Ch^2}{h+\varepsilon}$. Using the sup over all $\varepsilon \in (0,1]$, we get

$$
\sup_{\varepsilon\in(0,1]}\max_i \left|Z^{j+1}(s_i) - Z_i^{j+1}\right| \leq Ch. \tag{49}
$$

From the preceding theorem for the case when $\varepsilon > h$, the obtained scheme gives second-order uniformly convergent. For the case when $\varepsilon \ll h$, the scheme is first order uniformly convergent in spatial direction. □

Theorem 3. Let z and Z be the solutions of (2) and (35), respectively. Then we have the following uniform error bound:

$$\sup_{\varepsilon\in(0,1]} \left|z - Z\right| \leq C(h + (\Delta t)^2). \tag{50}$$

Proof. The proof can be done by the combination of Lemma 6 and Theorem 2. □

4 Numerical results and discussions

To show the applicability of the proposed method, two test examples are considered. Since the exact solutions of the examples are not known, we used a variant of the double mesh principle for the numerical inquiries. Therefore, we calculate, the maximum pointwise error by $E_\varepsilon^{N,M} = \max_{n,m}\left|Z_{n,m}^{N,M} - Z_{n,m}^{2N,2M}\right|$, the ε-uniform error by $E^{N,M} = \max_{n,m}(E_\varepsilon^{N,M})$, the rate of convergence by $r_\varepsilon^{N,M} = \log 2(E_\varepsilon^{N,M}/E_\varepsilon^{2N,2M})$, and the ε-uniform rate of convergence by $r^{N,M} = \log 2(E^{N,M}/E^{2N,2M})$.

Example 1. Consider the problem [3, 17] $\frac{\partial z}{\partial t} - \varepsilon\frac{\partial^2 z}{\partial s^2} + (2-s^2)\frac{\partial z}{\partial s} + sz(s,t) + z(s,t-\zeta) = 10t^2\exp(-t)s(1-s)$,
$(s,t) \in (0,1)\times(0,2]$ with interval condition $z(s,t) = 0$, on $(s,t) \in [0,1]\times[-1,0]$ and the boundary conditions $z(0,t) = 0$ and $z(1,t) = 0$, $t \in (0,2]$.

Example 2. Consider the problem [4, 17] $\frac{\partial z}{\partial t} - \varepsilon\frac{\partial^2 z}{\partial s^2} + (2-s^2)\frac{\partial z}{\partial s} + (s+1)(t+1)z(s,t) + z(s,t-\zeta) = 10t^2\exp(-t)s(1-s)$, $(s,t) \in (0,1)\times(0,2]$ with interval condition $z(s,t) = 0$, on $(s,t) \in [0,1]\times[-1,0]$ and the boundary conditions $z(0,t) = 0$, and $z(1,t) = 0$, $t \in [0,2]$.

The $E_\varepsilon^{N,M}$, $E^{N,M}$, and the corresponding $r^{N,M}$ of the proposed technique are revealed in Tables 1 and 3 for Examples 1 and 2, respectively, for different values of ε and N. These tables show that for every value of ε, the maximum absolute error monotonically decreases as the step sizes decrease, and as ε approaches zero, the maximum absolute error after getting

Table 1: $E_\varepsilon^{N,M}, E^{N,M}$, and $r^{N,M}$ for Example 1 for $\alpha_1 = 1/12$ and $\alpha_2 = 5/12$.

	Number of intervals $N = M$					
$\varepsilon \downarrow$	16	32	64	128	256	512
2^{-0}	5.0399e-04	1.5987e-04	5.6377e-05	2.2272e-05	9.6656e-06	4.3894e-06
2^{-2}	2.1240e-03	7.1347e-04	2.6592e-04	1.1006e-04	4.9294e-05	2.3209e-05
2^{-4}	3.9802e-03	1.3004e-03	4.8076e-04	1.9753e-04	8.7978e-05	4.1282e-05
2^{-6}	1.0244e-02	3.2295e-03	7.6535e-04	2.7318e-04	1.1175e-04	5.1015e-05
2^{-8}	1.1878e-02	5.7134e-03	2.4464e-03	7.8054e-04	1.8740e-04	6.6483e-05
2^{-10}	1.1882e-02	5.8162e-03	2.8862e-03	1.4139e-03	6.0782e-04	1.9424e-04
2^{-12}	1.1882e-02	5.8162e-03	2.8872e-03	1.4413e-03	7.2030e-04	3.5336e-04
2^{-14}	1.1882e-02	5.8162e-03	2.8872e-03	1.4413e-03	7.2055e-04	3.6032e-04
2^{-16}	1.1882e-02	5.8162e-03	2.8872e-03	1.4413e-03	7.2055e-04	3.6032e-04
2^{-18}	1.1882e-02	5.8162e-03	2.8872e-03	1.4413e-03	7.2055e-04	3.6032e-04
2^{-20}	1.1882e-02	5.8162e-03	2.8872e-03	1.4413e-03	7.2055e-04	3.6032e-04
$E^{N,M}$	1.1882e-02	5.8162e-03	2.8872e-03	1.4413e-03	7.2055e-04	3.6032e-04
$r^{N,M}$	1.0306	1.0104	1.0023	1.0002	0.99982	–

Table 2: $E^{N,M}$ and $r^{N,M}$ for Example 1 and results in [9, 12, 15, 27].

	Number of intervals N = M					
Schemes ↓	16	32	64	128	256	512
Proposed scheme						
$E^{N,M}$	1.1882e-02	5.8162e-03	2.8872e-03	1.4413e-03	7.2055e-04	3.6032e-04
$r^{N,M}$	1.0306	1.0104	1.0023	1.0002	0.99982	–
Results in [9]						
$E^{N,M}$	8.7361e-03	5.1124e-03	2.7590e-3	1.4328e-03	7.2999e-04	3.6844e-04
$r^{N,M}$	0.7730	0.8899	0.9453	0.9729	0.9865	–
Results in [27]						
$E^{N,M}$	1.0409e-02	4.9874e-03	2.6159e-03	1.4219e-03	7.3985e-04	3.7720e-04
$r^{N,M}$	1.0615	0.9310	0.8795	0.9425	0.9719	–
Results in [15]						
$E^{N,M}$	–	7.2307e-03	3.8523e-03	1.9892e-03	1.0107e-03	5.0944e-04
$r^{N,M}$	–	0.90842	0.95353	0.97683	0.98837	–
Result in [12]						
$E^{N,M}$	3.41e-02	1.84e-02	9.38e-03	4.67e-03	2.31e-03	1.15e-03
$r^{N,M}$	0.8901	0.9720	1.0062	1.0155	1.0063	–

Table 3: $E_\varepsilon^{N,M}$, $E^{N,M}$, and $r^{N,M}$ for Example 2 for $\alpha_1 = 1/12$ and $\alpha_2 = 5/12$.

	N=16	32	64	128	256	512
$\varepsilon \downarrow$	M=10	20	40	80	160	320
2^{-0}	8.1710e-04	3.5168e-04	1.6053e-04	7.6328e-05	3.7167e-05	1.8335e-05
2^{-2}	2.3598e-03	1.0816e-03	5.1201e-04	2.4851e-04	1.2233e-04	6.0677e-05
2^{-4}	2.9539e-03	1.4712e-03	7.3670e-04	3.6814e-04	1.8394e-04	9.1933e-05
2^{-6}	4.3251e-03	2.0366e-03	7.3922e-04	3.5960e-04	1.9129e-04	9.9512e-05
2^{-8}	4.1885e-03	2.4284e-03	1.3065e-03	5.6293e-04	1.9382e-04	9.0346e-05
2^{-10}	4.1877e-03	2.4165e-03	1.3326e-03	7.0702e-04	3.5310e-04	1.4638e-04
2^{-12}	4.1877e-03	2.4165e-03	1.3325e-03	7.0716e-04	3.6542e-04	1.8562e-04
2^{-14}	4.1877e-03	2.4165e-03	1.3325e-03	7.0716e-04	3.6542e-04	1.8591e-04
2^{-16}	4.1877e-03	2.4165e-03	1.3325e-03	7.0716e-04	3.6542e-04	1.8591e-04
2^{-18}	4.1877e-03	2.4165e-03	1.3325e-03	7.0716e-04	3.6542e-04	1.8591e-04
2^{-20}	4.1877e-03	1.9148e-03	1.3325e-03	7.0716e-04	3.6542e-04	1.8591e-04
$E^{N,M}$	4.1885e-03	2.4284e-03	1.3326e-03	7.0716e-04	3.6542e-04	1.8591e-04
$r^{N,M}$	0.7864	0.8658	0.9141	0.9525	0.9750	–

Table 4: $E^{N,M}$ and $r^{N,M}$ for Example 2 and results in [8, 9, 17, 20, 27].

Schemes $\downarrow$	N=16	32	64	128	256
	M=10	20	40	80	60
Proposed scheme					
$E^{N,M}$	4.1885e-03	2.4284e-03	1.3326e-03	7.0716e-04	3.6542e-04
$r^{N,M}$	0.7864	0.8658	0.9141	0.9525	0.9750
Results in[17]					
$E^{N,M}$	6.2345e-03	3.3323e-03	1.7040e-03	8.5888e-04	4.3092e-04
$r^{N,M}$	0.90376	0.96759	0.98840	0.99504	–
Results in [9]					
$E^{N,M}$	5.9184e-3	3.2992e-3	1.7387e-3	8.9106e-4	4.5088e-4
$r^{N,M}$	0.8431	0.9241	0.9644	0.9828	0.9915
Results in [27]					
$E^{N,M}$	5.4832e-03	3.3921e-03	1.8292e-03	9.4367e-04	4.7832e-04
$r^{N,M}$	0.6928	0.8910	0.9549	0.9803	0.9909
Results in [20]					
$E^{N,M}$	7.4252e-03	4.0993e-03	2.1528e-03	1.1033e-03	5.5845e-04
$r^{N,M}$	0.8570	0.9291	0.9644	0.9822	–
Results in [8]					
$E^{N,M}$	1.6119e-02	9.9504e-03	5.8541e-03	3.3439e-03	1.8650e-03
$r^{N,M}$	0.6960	0.7653	0.8079	0.8424	0.8660

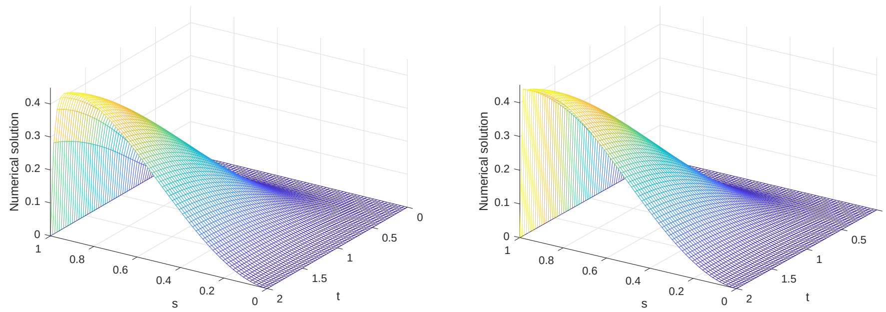

Figure 1: Numerical solution of Example 1 for $\varepsilon = 2^{-6}$ and $\varepsilon = 2^{-20}$, respectively.

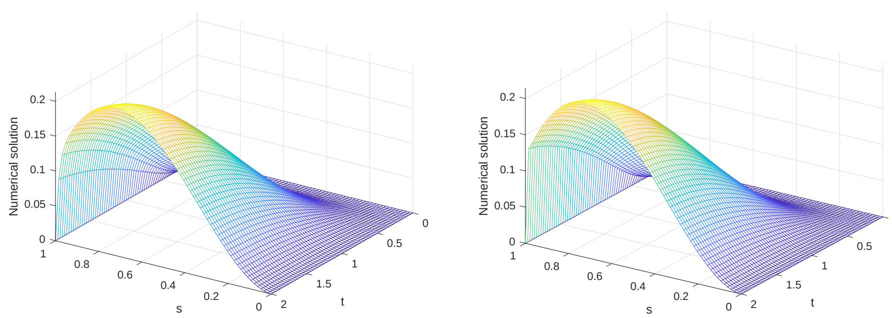

Figure 2: Numerical solution of Example 2 for $\varepsilon = 2^{-6}$ and $\varepsilon = 2^{-20}$, respectively.

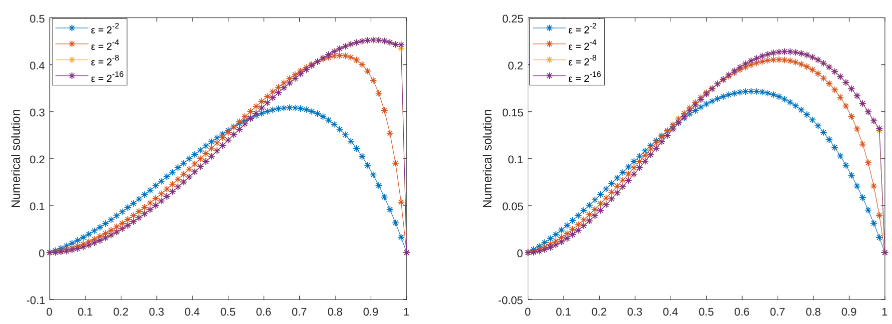

Figure 3: Effect of ε on solution profiles for Examples 1 and 2, respectively.

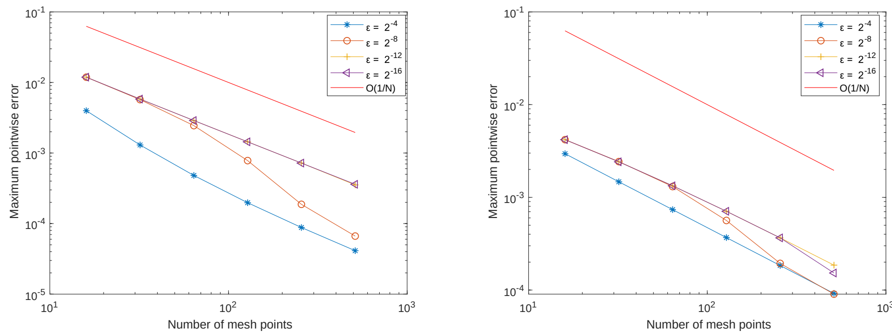

Figure 4: Maximum point wise error in Log-Log scale plot for Examples 1 and 2, respectively.

Table 5: $E_\varepsilon^{N,M}$ and $r_\varepsilon^{N,M}$

$\varepsilon\downarrow$	Example 1			Example 2		
	N=16	64	256	16	64	256
	M=16	32	64	16	32	64
2^{-8}	1.1878e-02	2.8201e-03	4.5728e-04	3.1525e-03	1.5003e-03	4.5534e-04
	2.0745	2.6246	–	1.0712	1.7202	–
2^{-10}	1.1882e-02	3.2531e-03	9.2321e-04	3.1516e-03	1.5299e-03	6.4765e-04
	1.8689	1.8171	–	1.0426	1.2402	–
2^{-12}	1.1882e-02	3.2540e-03	1.0390e-03	3.1516e-03	1.5298e-03	6.6540e-04
	1.8685	1.6470	–	1.0427	1.2010	–
2^{-14}	1.1882e-02	3.2540e-03	1.0393e-03	3.1516e-03	1.5298e-03	6.6541e-04
	1.8685	1.6466	–	1.0427	1.2010	–
2^{-16}	1.1882e-02	3.2540e-03	1.0393e-03	3.1516e-03	1.5298e-03	6.6541e-04
	1.8685	1.6466	–	1.0427	1.2010	–
2^{-18}	1.1882e-02	3.2540e-03	1.0393e-03	3.1516e-03	1.5298e-03	6.6541e-04
	1.8685	1.6466	-	1.0427	1.2010	–

large becomes constant, which demonstrates the ε-uniform convergence of the proposed scheme. On the other hand, the calculated $E^{N,M}$ and the corresponding $r^{N,M}$ using the proposed scheme are given in the last two rows, which confirms that the theoretical finding of the developed scheme is order one in the space direction. On the other hand, the results revealed in Table 5 confirm that the theoretical finding of the developed scheme is order two in the temporal direction. The comparison of the results of the developed method with the existing recently published works is revealed in Tables 2 and 4. From each table, one observed that the developed scheme outperforms existing methods.

The numerical solutions of the proposed scheme for each example are revealed in Figures 1 and 2. From Figures 1 and 2, it can be seen that a strong boundary layer is maintained along $s = 1$ as $\varepsilon \to 0$. Furthermore, to show the effect of ε on the steepness of the boundary layer the solutions are depicted in Figure 3. In each figure, we observe that as $\varepsilon \to 0$ the width of the boundary layers decreases, which confirms the desired result, that is, the boundary layer width of $O(\varepsilon)$. In addition, in Figure 4, the maximum pointwise errors of the scheme are plotted by the log-log scale. From these figures, one can observe that maximum absolute error decreases as the step sizes decrease for every value of ε, which confirms the ε-uniform convergence of the proposed scheme.

5 Conclusion

In this study, we initiated a fitted tension spline numerical scheme for a singularly perturbed parabolic problem with a large temporal lag. The solution to the problem exhibited a boundary layer on the right side of the domain. The proposed scheme comprises the Crank–Nicolson method in the time direction and an exponentially fitted tension spline scheme in the spatial direction. The efficiency and applicability of the developed scheme are validated. The computational results are tabulated in terms of $E_\varepsilon^{N,M}$, $E^{N,M}$, and the corresponding $r^{N,M}$. The effect of ε on the steepness of the boundary layer is revealed graphically. Furthermore, the computational results are compared with some of the existing literature and the obtained scheme outperforms existing methods. The proposed method contributes a more accurate, stable, and ε-uniform numerical result with a linear order of convergence in space and second-order convergence in time. The proposed scheme can be extended for singularly perturbed turning point problems.

Acknowledgements

The authors thank in advance the editor and reviewers for their constructive comments.

References

[1] Ansari, A.R., Bakr, S.A. and Shishkin, G.I. *A parameter-robust finite difference method for singularly perturbed delay parabolic partial differential equations*, J. Comput. and Appl. Math. 205(1) (2007), 552–566.

[2] Babu, G. and Bansal, K. *A high order robust numerical scheme for singularly perturbed delay parabolic convection diffusion problems*, J. Appl. Math. Comput. 68(1) (2022), 363–389.

[3] Das, A. and Natesan, S. *Uniformly convergent hybrid numerical scheme for singularly perturbed delay parabolic convection–diffusion problems on Shishkin mesh*, Appl. Math. Comput. 271 (2015), 168–186.

[4] Das, A. and Natesan, S. *Second-order uniformly convergent numerical method for singularly perturbed delay parabolic partial differential equations*, Int. J. Comput. Math. 95(3) (2018), 490–510.

[5] Ejere, A.H., Dinka, T.G., Woldaregay, M.M. and Duressa, G.F. *A tension spline fitted numerical scheme for singularly perturbed reaction-diffusion problem with negative shift*, BMC Res. Notes. 16(1) (2023), 112.

[6] Ejere, A.H., Duressa, G.F., Woldaregay, M.M. and Dinka, T.G. *A robust numerical scheme for singularly perturbed differential equations with spatio-temporal delays*, Front. Appl. Math. Stat. 9 (2023), 1125347.

[7] Govindarao, L. and Mohapatra, J. *A second order numerical method for singularly perturbed delay parabolic partial differential equation*, Eng. Comput. 36(2) (2018), 420–444.

[8] Gowrisankar, S. and Natesan, S. *ε-Uniformly convergent numerical scheme for singularly perturbed delay parabolic partial differential equations*, Int. J. Comput. Math. 94(5) (2017), 902–921.

[9] Hassen Z.I. and Duressa, G.F. *New approach of convergent numerical method for singularly perturbed delay parabolic convection-diffusion problems*, Res. Math. 10(1) (2023), 1–14.

[10] Kellogg, R.B. and Tsan, A. *Analysis of some difference approximations for a singular perturbation problem without turning points*, Math. Comp. 32(144) (1978), 1025–1039.

[11] Khan, I. and Tariq, A. *Tension spline method for second-order singularly perturbed boundary-value problems*, Int. J. Comput. Math. 82(12) (2005), 1547–1553.

[12] Kumar, D. and Kumari, P. *A parameter-uniform numerical scheme for the parabolic singularly perturbed initial boundary value problems with large time delay*, J. Appl. Math. Comput. 59(1-2) (2019), 179–206.

[13] Kumar, K., Gupta, T., Chakravarthy, P.P. and Rao, R.N. *An adaptive mesh selection strategy for solving singularly perturbed parabolic partial differential equations with a small delay*, Appl. Math. Sci. Comput. (2019) 67–76.

[14] Kumar, K., Podila, P.C., Das, P. and Ramos, H. *A graded mesh refinement approach for boundary layer originated singularly perturbed time-delayed parabolic convection diffusion problems*, Math. Methods Appl. Sci. 44(16) (2021), 12332–12350.

[15] Negero, N.T. and Duressa, G.F. *An efficient numerical approach for singularly perturbed parabolic convection-diffusion problems with large time-lag*, J. Math. Model. (2021), 1–18.

[16] Negero, N.T. and Duressa, G.F. *A method of line with improved accuracy for singularly perturbed parabolic convection-diffusion problems with large temporal lag*. Results Appl. Math. 11 (2021), 100–174.

[17] Negero, N.T. and Duressa, G.F. *Uniform Convergent Solution of Singularly Perturbed Parabolic Differential Equations with General Temporal-Lag*, Iran. J. Sci. Technol. Trans. A Sci. (2022), 1–18.

[18] O'malley, R.E. *Singular perturbation methods for ordinary differential equations*, Springer, 1991, 89.

[19] Oruç, Ö. *A non-uniform Haar wavelet method for numerically solving two-dimensional convection-dominated equations and two-dimensional near singular elliptic equations*, Comput. Math. with Appl. 77(7) (2019), 1799–1820.

[20] Podila, P.C. and Kumar, K. *A new stable finite difference scheme and its convergence for time-delayed singularly perturbed parabolic PDES*, Comput. Appl. Math. 39(3) (2020), 1–16.

[21] Protter M. and Weinberger, H. *Maximum principles in differential equations*, Englewood Cliffs, New Jersey: Prentice-Hall Inc. 1967.

[22] Sahoo, S.K. and Gupta, V. *Parameter robust higher-order finite difference method for convection-diffusion problem with time delay*, Numer. Methods Partial. Differ. Equ. 39(6) (2023), 4145–4173.

[23] Salama, A. and Al-Amery, D. *A higher order uniformly convergent method for singularly perturbed delay parabolic partial differential equations*, Int. J. Comput. Math. 94(12) (2017), 2520–2546.

[24] Shishkin, G.I. and Shishkina, L.P. *Difference methods for singularly perturbed problems*, CRC, 2008.

[25] Tesfaye, S.K., Woldaregay, M.M., Dinka, T.G. and Duressa, G.F. *Fitted computational method for solving singularly perturbed small time lag problem*, BMC Res. Notes. 15(1) (2022), 1–10.

[26] Wang, P.K.C. *Asymptotic stability of a time-delayed diffusion system*, (1963) 500–504.

[27] Woldaregay, M.M., Aniley, W.T. and Duressa, G.F. *Novel numerical scheme for singularly perturbed time delay convection-diffusion equation*, Adv. Math. Phys. 2021 (2021).